Effect of Chain Architecture on Biaxial Orientation and Oxygen Permeability of Polypropylene Film

P. Dias,[1] Y. J. Lin,[1] A. Hiltner,[1] E. Baer,[1] H. Y. Chen,[2] S. P. Chum[2]

[1]*Department of Macromolecular Science and Engineering, Center for Applied Polymer Research, Case Western Reserve University, Cleveland, Ohio 44106-7202*
[2]*Polyolefins and Elastomers R&D, The Dow Chemical Company, Freeport, Texas 77541*

Received 31 July 2007; accepted 24 August 2007
DOI 10.1002/app.27197
Published online 25 October 2007 in Wiley InterScience (www.interscience.wiley.com).

ABSTRACT: Films of two isotactic propylene homopolymers prepared with different catalysts and a propylene/ethylene copolymer were biaxially oriented under conditions of temperature and strain rate that were similar to those encountered in a commercial film process. The draw temperature was varied in the range between the onset of melting and the peak melting temperature. It was found that the stress response during stretching depended on the residual crystallinity in the same way for all three polymers. Biaxial orientation reduced the oxygen permeability of the oriented films, however, the reduction did not correlate with the amount of orientation as measured by birefringence, with the fraction of amorphous phase as determined by density, or with free volume hole size as determined by PALS. Rather, the decrease in permeability was attributed to reduced mobility of amorphous tie molecules. A single one-to-one correlation between the oxygen permeability and the intensity of the dynamic mechanical β-relaxation was demonstrated for all the polymers used in the study. © 2007 Wiley Periodicals, Inc. J Appl Polym Sci 107: 1730–1736, 2008

Key words: polypropylene; biaxial orientation; oxygen permeability

INTRODUCTION

Polypropylene is a candidate material for packaging applications because of its low cost and good thermal stability. Other key requirements for beverage and food packaging are atmosphere control and mechanical robustness. Commercial polypropylene films are typically oriented to enhance the toughness. A tentering process is used in which the extruded film is quenched, reheated, and rapidly biaxially drawn either in a single step or sequentially. The biaxial drawing is typically performed at temperatures intermediate between the onset of melting and the peak melting temperature.[1–3] Drawing at lower temperatures requires larger forces and often results in void formation. With increasing temperature, the stress-response decreases as the crystalline phase starts to melt.[4] However, the tie chains become less effective as the anchoring crystals melt, with the result that too high a drawing temperature gives rise to lower molecular orientation.[5,6]

Most studies that probe the relationship between orientation and the solid state properties focus on uniaxially oriented polypropylene. Several reports demonstrate a correlation between the modulus and the total crystalline and amorphous phase orientation.[5,7] Orientation also reduces the gas permeability of polypropylene.[8] The relationship between orientation and gas permeability is not well understood. Permeability does not exhibit a simple relationship with optical birefringence, which reflects the total combined molecular orientation of the crystalline and amorphous phases.[9] However, it should be noted that one report, with very limited data, showed a correlation between oxygen permeability and Herman's amorphous phase orientation function in the transport direction.[10]

More recently, the decrease in permeability of a propylene copolymer was specifically identified with decreased diffusivity, the dynamic component of permeability.[8] Decreased mobility of the oriented amorphous chains was thought to be responsible. The molecular mobility of amorphous chains can be characterized by the dynamic mechanical relaxation behavior. In a family of copolyesters, a strong correlation was found between oxygen diffusivity and the intensity of the subambient γ-relaxation peak.[11] In polypropylene, main chain motions in the amorphous phase are associated with the β-relaxation. It has been shown that orientation decreases the intensity of the β-relaxation.[12,13] However, a direct correlation with gas permeability has not been established.

Advances in catalyst technology make it possible to synthesize polypropylenes and propylene copolymers that differ substantially in molecular weight

Correspondence to: A. Hiltner (ahiltner@case.edu).
Contract grant sponsor: The Dow Chemical Company.

Journal of Applied Polymer Science, Vol. 107, 1730–1736 (2008)

and molecular weight distribution, in stereo defect type and distribution, and in comonomer distribution. It has been suggested that this unprecedented control of the molecular structure can lead to a set of differentiated properties of oriented film.[1,14,15] In the present study, three isotactic polypropylene resins that differed in the chain architecture were biaxially oriented at various temperatures close to the peak melting temperature. The relationship between the extent of melting and the processability was explored. In addition, correlations were sought between the oxygen permeability of the biaxially oriented films and the amorphous chain mobility.

EXPERIMENTAL

Two homopolymers and a copolymer were supplied by The Dow Chemical Company. The two homopolymers were a commercial Ziegler-Natta polypropylene (DOW 5D98) and a new developmental polypropylene. The Ziegler-Natta polypropylene is referred to as ZN-PP, and the developmental polypropylene is referred to as D-PP. The propylene–ethylene copolymer was a commercial grade Ziegler-Natta propylene-ethylene copolymer (DOW 6D20) that was chosen to have a similar peak melting temperature as D-PP. It is referred to as ZN-P/E.

The D-PP was prepared with a post-metallocene catalyst. It had weight average molecular weight M_w of 3.42×10^5 g mol^{-1} and M_w/M_n of 2.9 as determined by gel permeation chromatography calibrated with polystyrene standards. The equivalent polypropylene molecular weights were deduced using appropriate Mark-Houwink coefficients for polypropylene and polystyrene.

Unoriented sheets with a thickness of $\sim$ 0.6 mm were prepared by compression molding. Pellets were sandwiched between Mylar® sheets and preheated at 190°C under minimal pressure for 8 min and then compressed at 10 MPa for 5 min using a Model 3912 laboratory press, Carver (Wabash, IN) before quenching.

Thermal analysis was performed on the sheets using a Perkin-Elmer (Boston, MA) DSC-7 calorimeter under a nitrogen atmosphere. Samples weighing 5–10 mg were cut from the molded sheets, and thermograms were obtained at a heating rate of 10°C min^{-1} from -60 to 190°C. The percent crystallinity was calculated using a value of $\Delta H = 209$ J g^{-1} for the heat of fusion of 100% crystalline isotactic PP.[16]

Specimens measuring 85 mm $\times$ 85 mm were cut from the compression molded sheets, marked with a square grid pattern, and loaded into a Karo IV Biaxial Stretcher, Brückner (Greenville, SC). The sheets were simultaneously and equi-biaxially drawn at the various temperatures indicated by arrows in Figure 1, and to draw ratios of 5 $\times$ 5, 6 $\times$ 6, 7 $\times$ 7, and 8 $\times$ 8 at an engineering strain rate of 400% s^{-1} based on the original specimen dimensions. The preheat time before drawing was fixed at 1 min. Load and displacement were recorded and stress–strain curves were calculated from these data. The uniformity of the drawn specimen was determined from the even deformation of the grid pattern.

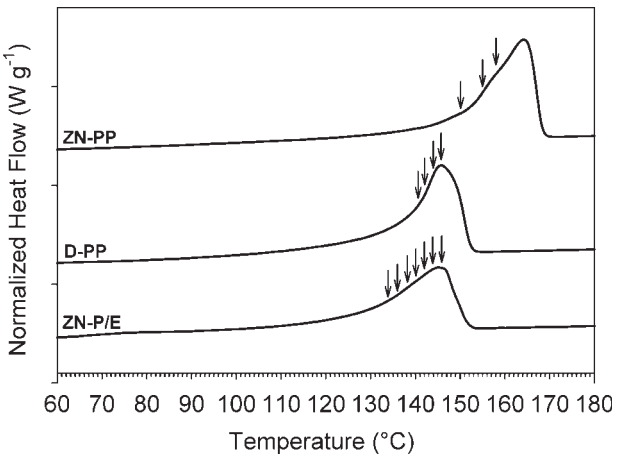

Figure 1 Melting thermograms of ZN-PP, D-PP, and ZN-P/E molded sheets. Arrows indicate the temperatures at which the sheets were successfully biaxially drawn.

The DSC was used to estimate the residual crystallinity at the draw temperature. Specimens were heated to the draw temperature at 80°C min^{-1} and held isothermally at the draw temperature for 1 min and subsequently heated at 10°C min^{-1} to 190°C. The residual crystallinity was calculated from the endotherm in the second heating stage between the isothermal draw temperature and 190°C.

Density was measured at 23°C according to ASTM D1505-85. A 2-propanol/water gradient column with a density range of 0.85–0.95 g cm^{-3} was calibrated with glass floats of known density. Small pieces of samples $\sim$ 2 $\times$ 2 mm^2 were placed in the column and allowed to equilibrate for 10 h before measurement. The reported density is the average of at least three specimens and has an error of less than 0.0005 g cm^{-3}.

Oxygen flux *J(t)* at 0% relative humidity, 1 atm and 23°C was measured with a Mocon (Minneapolis, MN) OX-TRAN 2/20. Oxygen permeability $P(O_2)$ was obtained from the steady state flux J as

$$P(O_2) = Jl/p \quad (1)$$

where p is the pressure and l is the film thickness.

Dynamic mechanical thermal analysis (DMTA) of oriented films was carried out with a Polymer Laboratories (Boston, MA) Dynamic Mechanical Thermal Analyzer. Specimens were tested in the dynamic tensile mode with a frequency of 1 Hz and a strain of 0.085% from -60 to 120°C with a heating rate of 3°C min^{-1} and a grip to grip distance of 13.0 mm.

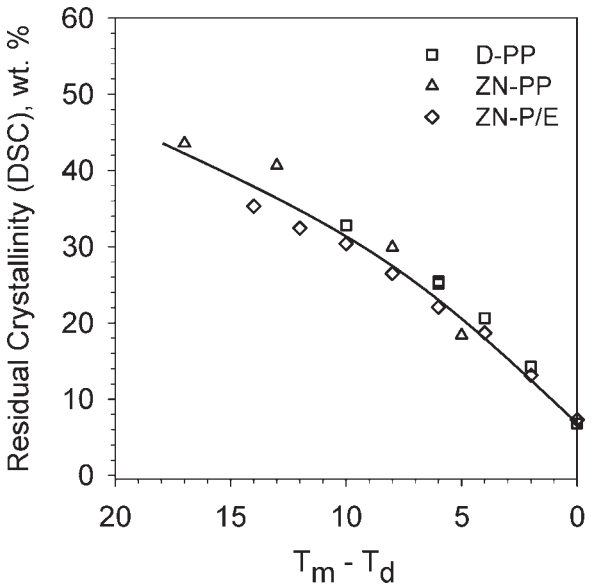

Figure 2 Effect of undercooling $T_m - T_d$ on the residual crystallinity X_c of D-PP, ZN-PP, and ZN-P/E.

To determine free-volume hole size, positron annihilation lifetime spectroscopy (PALS) was performed using a conventional fast–fast coincidence system. The instrumentation and procedure for data analysis were described previously.[17]

RESULTS AND DISCUSSION

Biaxial orientation

The DSC thermograms for ZN-PP, D-PP, and ZN-P/E are shown in Figure 1. The melting peaks for the three materials were 165, 147, and 144°C, respectively. The lower melting temperature of D-PP compared to ZN-PP was attributed to differences in defect population and distribution, which resulted in shorter isotactic runs when compared with the ZN-PP. The D-PP was substantially isotactic and had at least 50% more regio-errors than a comparable ZN-PP polypropylene.[18] However, D-PP and ZN-PP had essentially the same heat of melting, 92 J g^{-1} (56% crystallinity) and 93 J g^{-1} (56% crystallinity), respectively. The copolymer ZN-P/E was chosen to have a melting temperature similar to that of D-PP. Although the peak melting temperature was about the same for the two resins, the melting endotherm of ZN-P/E was much broader, and the heat of melting was lower, 84 J g^{-1} (51% crystallinity), due to the additional chain defects imparted by comonomer units.

The residual crystallinity, defined as the amount of crystallinity remaining at the draw temperature, is shown in Figure 2. The data for the three polymers collapsed to a single line when plotted as a function of undercooling regardless of chain architecture. The processability of the three polymers was tested and compared in the temperature range between the onset of melting and the peak melting temperature.

The stress–strain experiments were terminated when the force exceeded the limit of the instrument grips (approximately 100 N) or when the displacement reached the limit of the instrument (10 × 10). Typical biaxial stress–strain curves are presented in Figure 3. All the polymers exhibited yielding, as indicated by a maximum in the engineering stress–strain curve, followed by a plateau region of con-

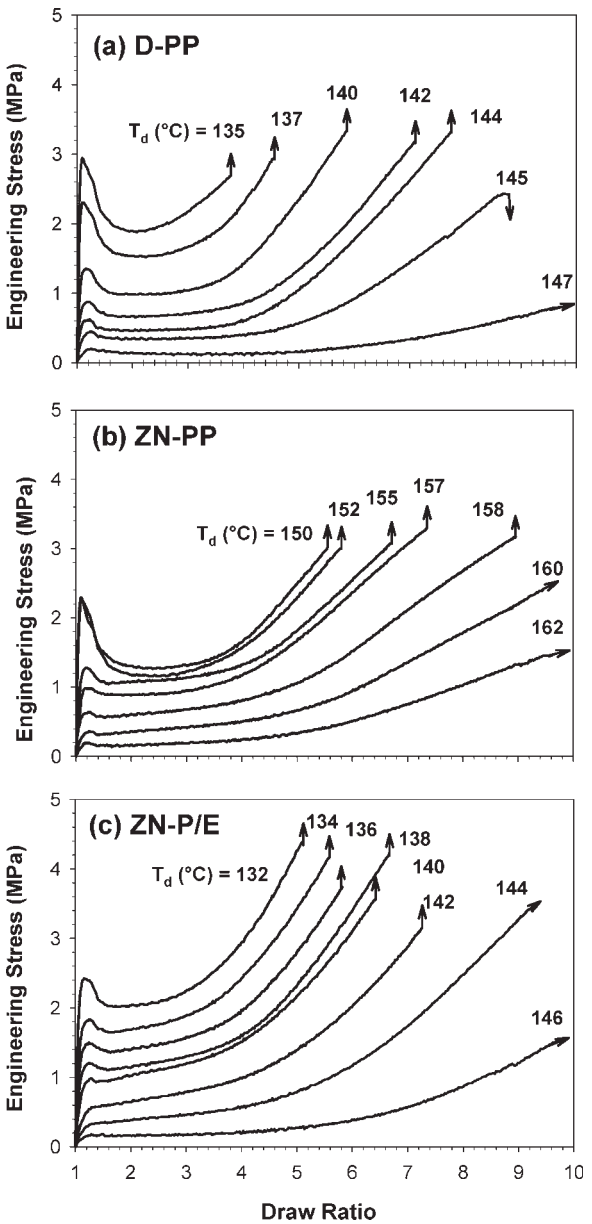

Figure 3 Effect of biaxial drawing temperature T_d on the stress response of: (a) D-PP; (b) ZN-PP; and (c) ZN-P/E. Upward pointing arrows indicate where the experiment was terminated when the force exceeded the capability of the instrument. Downwards pointing arrows indicate film fracture.

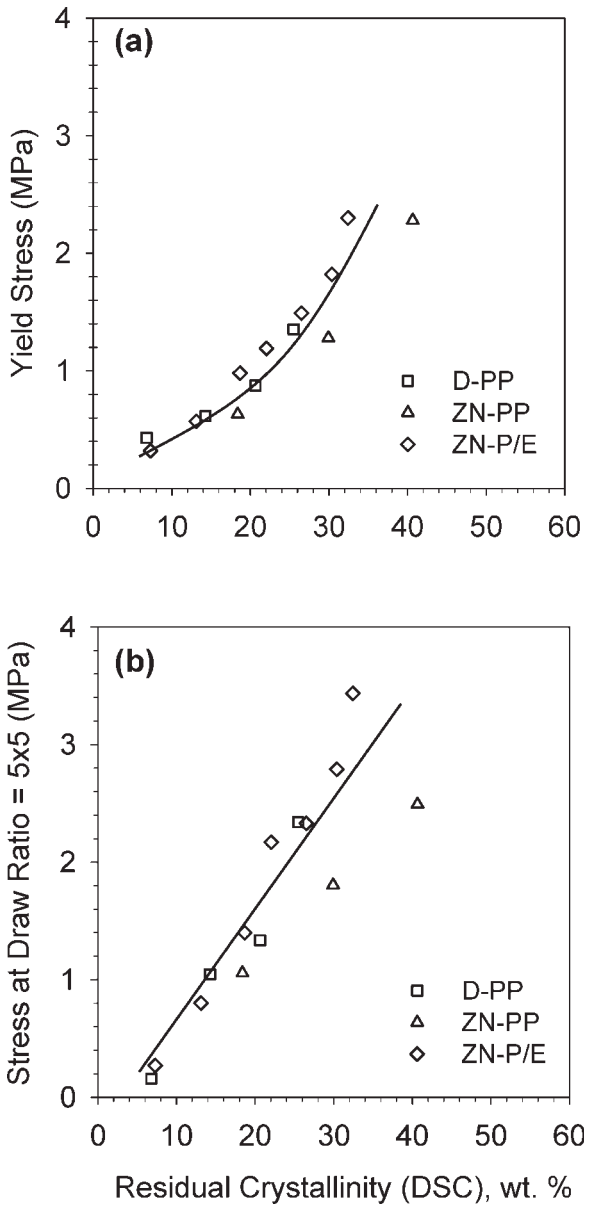

Figure 4 Effect of residual crystallinity X_c on: (a) yield stress; and (b) stress at a draw ratio of 5 × 5.

stant stress. As the draw temperature increased, and more of the polymer was in the melt, both the yield stress and the plateau draw stress dropped. Substantial strain hardening was observed at all draw temperatures except for the highest, although the onset of strain hardening occurred at a higher strain as the draw temperature increased. As a consequence, the stress that the film experienced when it was drawn to some target draw ratio decreased as the draw temperature was raised.

The effect of increasing temperature was to reduce the amount of crystallinity through partial melting. However, the yield stress depended on the residual crystallinity in the same way for all the polymers regardless of the chain architecture, Figure 4 (a). Similarly, the relationship between the stress at a draw ratio of 5 × 5 and the residual crystallinity was approximately the same for all the polymers, Figure 4(b). Although all the resins could be drawn over a fairly large temperature range, the results were not always considered successful. The criterion for successful drawing was achieving a draw ratio of at least 5 × 5 with good uniformity of the drawn films as indicated by uniform deformation of a stamped-on square grid pattern. Good uniformity as judged by eye was confirmed by uniform birefringence over a circular area with a 30 cm diameter in the center of the film. Because of necking of the films during stretching, uniform films with draw ratios less than the natural draw ratio of about 5 × 5 could not be achieved at any temperature. The high temperature end of the process window was defined as the highest temperature at which specimens drew uniformly to at least 5 × 5. The lowest temperature at which the film could be drawn to 5 × 5 without exceeding the load limit of the grips defined the low temperature end of the process window for films of the thickness used in this study. To meet this condition, the residual crystallinity had to be 40 wt % or less for the film thickness used in this study.

Oxygen permeability

The orientation of the stretched films was described by the birefringence, defined as

$$\Delta n = \frac{n_x + n_y}{2} - n_z \tag{2}$$

where n_x and n_y are the refractive indices in the two stretching directions and n_z is the refractive index in

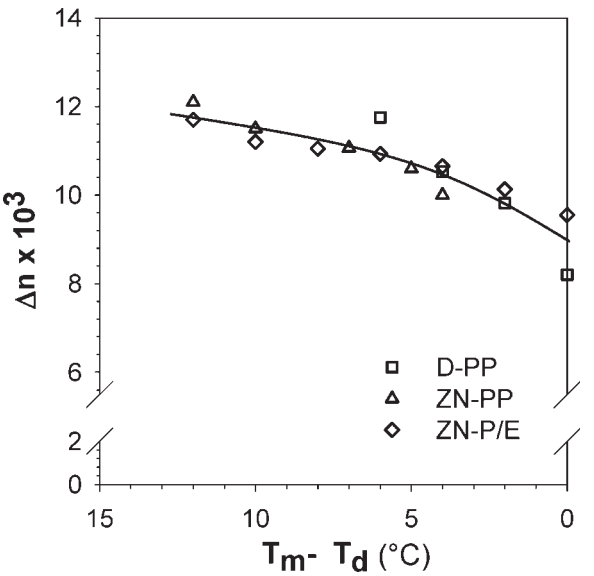

Figure 5 Figure 5 Relationship between undercooling $T_m - T_d$ and the birefringence Δn of drawn films.

TABLE I
Refractive Index and Tensile Modulus of Polypropylene Films

Polymer	Draw ratio	T_d (°C)	$T_m - T_d$ (°C)	n_x	n_y	n_z	Δn ($\times 10^3$)	Modulus, 2% secant (MPa)	Modulus, 20% secant (MPa)
D-PP	1×1	–		1.5029 ± 0.0001	1.5029 ± 0.0001	1.5029 ± 0.0001	0.0	1000	90
D-PP	5×5	145	1	1.5097 ± 0.0002	1.5101 ± 0.0001	1.4911 ± 0.0001	8.1	1300	250
D-PP	5×5	144	2	1.5083 ± 0.0001	1.5079 ± 0.0001	1.4911 ± 0.0001	9.8	1400	330
D-PP	5×5	142	4	1.5108 ± 0.0005	1.5096 ± 0.0001	1.4882 ± 0.0002	10.5	1400	360
D-PP	5×5	140	6	1.5094 ± 0.0005	1.5087 ± 0.0001	1.4876 ± 0.0010	11.7	1600	440
ZN-PP	1×1	–		1.5066 ± 0.0001	1.5066 ± 0.0001	1.5066 ± 0.0001	0.0	900	100
ZN-PP	5×5	158	5	1.5100 ± 0.0004	1.5100 ± 0.0002	1.5000 ± 0.0001	10.0	1200	410
ZN-PP	5×5	155	8	1.5106 ± 0.0004	1.5104 ± 0.0005	1.4994 ± 0.0001	11.1	1600	440
ZN-PP	5×5	150	13	1.5087 ± 0.0001	1.5094 ± 0.0001	1.4982 ± 0.0001	12.1	1500	440
ZN-P/E	1×1	–		1.5066 ± 0.0001	1.5066 ± 0.0001	1.5066 ± 0.0001	0.0	800	85
ZN-P/E	5×5	144	2	1.5100 ± 0.0008	1.5100 ± 0.0006	1.5005 ± 0.0005	9.5	900	280
ZN-P/E	5×5	140	6	1.5100 ± 0.0006	1.5100 ± 0.0004	1.4993 ± 0.0003	10.7	1100	375
ZN-P/E	5×5	136	10	1.5100 ± 0.0004	1.5100 ± 0.0002	1.4989 ± 0.0001	11.1	1100	370
ZN-P/E	5×5	132	14	1.5087 ± 0.0001	1.5094 ± 0.0001	1.4985 ± 0.0001	11.7	1600	470

the normal direction.[2,5,9] The quantity Δn is plotted against the undercooling ($T_m - T_d$) for biaxially drawn 5 × 5 films in Figure 5. The values for oriented films prepared from the three polymers all fell in the same range. The gradual decrease in Δn as T_d approached T_m reflected relaxation of the amorphous tie chains as more of the anchoring crystals melted. The modulus of the biaxially drawn films increased substantially with increasing birefringence, Table I. This result has been attributed to an increase in amorphous and crystalline phase orientation.[7]

Biaxial orientation decreased the oxygen permeability $P(O_2)$ of the polypropylene films, Table II. However, there was no consistent correlation with the amount of orientation as measured by Δn. For example, $P(O_2)$ of the D-PP films was not affected by orientation unless Δn exceeded a value of about 10. On the other hand, ZN-PP could not be uniformly drawn to Δn less than 10, and $P(O_2)$ was independent of Δn for values between 10 and 12. In contrast, ZN-PE showed a gradual decrease in $P(O_2)$ with increasing Δn. A previous study also did not find a simple correlation between $P(O_2)$ and Δn for uniaxially oriented ZN-P/E, and similarly found that relatively high levels of orientation as measured by Δn were required before a significant decrease in $P(O_2)$ occurred.[9] In addition, no correlation was found between $P(O_2)$ and n_z, which is a measure of the orientation in the thickness direction, i.e. the direction of gas transport.

The refractive indices combine contributions from the crystalline and amorphous phases. However, gas transport is generally assumed to occur only in the amorphous phase. The permeability is the product of the solubility S and the diffusivity D. The solubility is determined by the amount of the amorphous phase and the free volume of the amorphous phase. Density provided a measure of the amount of amorphous phase. Although the density initially increased with orientation, which was consistent with lower $P(O_2)$, Table II, the steady decrease in density thereafter was not reflected by a corresponding increase in P.

TABLE II
Properties of Polypropylene Films

Polymer	Draw ratio	T_d (°C)	$T_m - T_d$ (°C)	Density (g cm^{-3})	$P(O_2)$ (barrers)	$\langle v_h \rangle$ (Å^3)
D-PP	1×1	–	–	0.9001 ± 0.0003	0.97 ± 0.02	114 ± 2
D-PP	5×5	145	1	0.9079 ± 0.0002	0.94 ± 0.03	109 ± 3
D-PP	5×5	144	2	0.9078 ± 0.0002	0.94 ± 0.02	108 ± 3
D-PP	5×5	142	4	0.9075 ± 0.0002	0.84 ± 0.03	110 ± 3
D-PP	5×5	140	6	0.9060 ± 0.0002	0.72 ± 0.03	109 ± 4
ZN-PP	1×1	–	–	0.8999 ± 0.0002	0.91 ± 0.02	120 ± 4
ZN-PP	5×5	158	5	0.9112 ± 0.0002	0.77 ± 0.02	117 ± 3
ZN-PP	5×5	155	8	0.9073 ± 0.0002	0.73 ± 0.00	113 ± 3
ZN-PP	5×5	150	13	0.9073 ± 0.0002	0.73 ± 0.02	111 ± 3
ZN-P/E	1×1	–	–	0.8946 ± 0.0001	1.35 ± 0.02	121 ± 3
ZN-P/E	5×5	144	2	0.9053 ± 0.0001	1.07 ± 0.03	112 ± 4
ZN-P/E	5×5	140	6	0.9040 ± 0.0001	1.02 ± 0.02	109 ± 4
ZN-P/E	5×5	136	10	0.9027 ± 0.0004	0.94 ± 0.02	108 ± 5
ZN-P/E	5×5	132	14	0.9002 ± 0.0001	0.91 ± 0.02	113 ± 3

The free volume hole size $\langle v_h \rangle$ as measured by PALS was slightly smaller in the biaxially oriented films than in the unoriented control film, which was consistent with lower P, Table II. However, there was little variation in hole size among the various oriented films, indicating that the free volume hole size did not correlate with P. Thus, it was concluded that any changes in S were too small to be significant, and the effect of biaxial orientation on P should be sought in changes to D.

A relationship between D and the mobility of the amorphous chain segments as measured by the strength of dynamic mechanical relaxations that occur below the test temperature has been demonstrated in some polymers.[11] The dynamic mechanical β-relaxation peak of polypropylene at about 10°C corresponds to the glass transition temperature and is related to segmental mobility of the amorphous chains. The β-relaxation overlaps the onset of the crystalline α-relaxation. Thus, to the obtain the intensity of the β-relaxation, the tan δ curve was deconvoluted into three Gaussian contributions from the β-relaxation, the α-relaxation, and the onset of melting, respectively, Figure 6. The intensity of the β-relaxation was taken as the height of the deconvoluted peak.

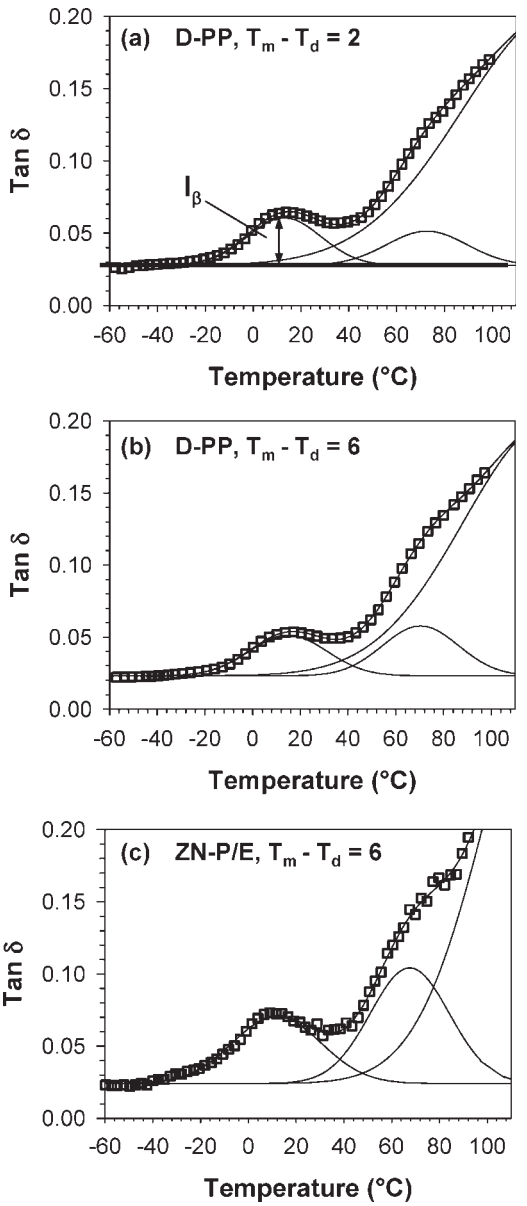

Figure 6 DMTA tan δ curves deconvoluted into three Gaussian contributions for the β-relaxation, α-relaxation, and the onset of melting. The solid line through the data points is the summation of the three contributions.

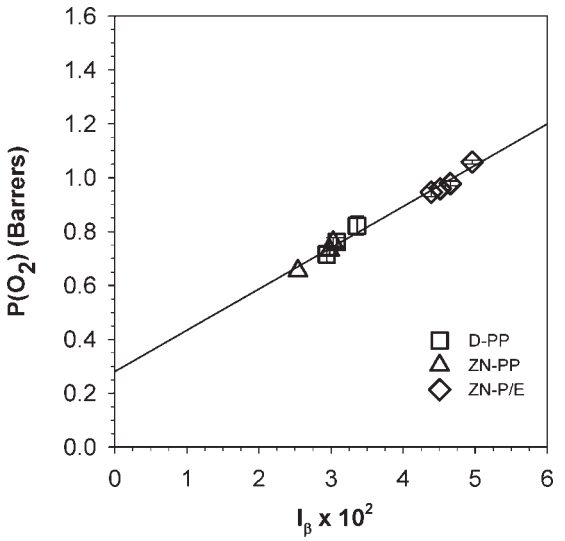

Figure 7 Dependence of the oxygen permeability $P(O_2)$ at 23°C on the intensity of the deconvoluted DMTA β-relaxation I_β.

A very strong correlation was found between the intensity of the deconvoluted β-relaxation and $P(O_2)$ as shown in Figure 7. A single correlation was found for all the polymers. Thus, it appeared that $P(O_2)$ depended on the mobility of the amorphous phase chains. It is imagined that the process of orienting the partially crystalline film stretched and tightened the tie molecules that connected the crystals and transferred the stress. The reduced mobility of the tie chains, as measured by the intensity of the β-relaxation, resulted in a lower D. This effect was the major influence on P of the biaxially oriented films at 23°C. Extrapolation of the least-squares regression fit to zero β-relaxation intensity yielded $P(O_2)$ of 0.28 Barrers. It was expected that sub-T_g relaxations allowed for some chain mobility and oxygen permeation below T_g.

CONCLUSIONS

Two isotactic propylene homopolymers prepared from different catalysts and a propylene/ethylene

copolymer were compared in this study of biaxially oriented film. Orientation was performed under conditions of temperature and strain rate that were similar to those encountered in a commercial film process. Biaxial orientation reduced the oxygen permeability of the oriented films, however, the reduction did not correlate with the amount of orientation as measured by birefringence, with the fraction of amorphous phase as determined by density, or with the free volume hole size as determined by PALS. Rather, the decrease in permeability was attributed to reduced mobility of amorphous tie molecules. A single one-to-one correlation between the oxygen permeability and the intensity of the dynamic mechanical β-relaxation was demonstrated for all the polymers used in the study.

The authors thank The Dow Chemical Company for generous technical support.

References

1. Phillips, R. A.; Nguyen, T. J Appl Polym Sci 2001, 80, 2400.
2. Dias, P.; Hiltner, A.; Baer, E.; Van Dun, J.; Chen, H. Y.; Chum, S. P. Annu Tech Conf Soc Plast Eng 2006, 64, 2660.
3. Lupke, T.; Dunger, S.; Sanze, J.; Radusch, H. Polymer 2004, 45, 6861.
4. Rettenberger, S.; Capt, L.; Munstedt, H.; Stopperka, K.; Sanze, J. Rheol Acta 2002, 41, 332.
5. Samuels, R. J. Structured Polymer Properties: The Identification, Interpretation, and Application of Crystalline Polymer Structure; Wiley-Interscience: New York, 1974.
6. Loos, J.; Schimanski, T. Macromolecules 2005, 38, 10678
7. Yamada, K.; Kamezawa, M.; Takayanagi, M. J Appl Polym Sci 1981, 26, 49.
8. Somlai, L. S.; Liu, R. Y. F.; Landoll, L. M.; Hiltner, A.; Baer, E. J Polym Sci B 2005, 43, 1230.
9. Taraiya, A. K.; Orchard, G. A. J.; Ward, I. M. J Appl Polym Sci 1990, 41, 1659.
10. Taraiya, A. K.; Orchard, G. A. J.; Ward, I. M. J Polym Sci B 1993, 31, 641.
11. Polyakova, A.; Liu, R. Y. F.; Schiraldi, D. A.; Hiltner, A.; Baer, E. J Polym Sci B 2001, 39, 1889.
12. Wills, A. J.; Capaccio, G.; Ward, I. M. J Polym Sci B 1980, 18, 493.
13. Elias, M. B.; Machado, R. J Therm Anal Cal 2000, 59, 143.
14. Lin, C. Y.; Chen, M. C.; Mehta, A. K. J Plast Films Sheeting 2001, 17, 113.
15. DeMeuse, M. T. J Plastic Film Sheeting 2002, 18, 17.
16. Brandrup, J.; Immergut, E. H. Polymer Handbook, 3rd ed.; Wiley: New York, 1989.
17. Higuchi, H.; Yu, Z.; Jamieson, A. M.; Simha, R.; McGervey, J. D. J Polym Sci B 1995, 33, 2295.
18. Tau, L. M.; Chum, S. P. W.; Karande, S.; Bosnyak, C. U.S. Pat. 7,041,765 B2 (2006).